

Megagauss Magnetic Field Generation and Plasma Jet Formation on Solid Targets Irradiated by an Ultraintense Picosecond Laser Pulse

M. Borghesi, A. J. MacKinnon, A. R. Bell, R. Gaillard, and O. Willi

The Blackett Laboratory, Imperial College of Science, Technology and Medicine, London SW7 2BZ, United Kingdom

(Received 20 May 1997)

The spatial and temporal evolution of spontaneous megagauss magnetic fields, generated during the interaction of a picosecond pulse with solid targets at irradiances above 5×10^{18} W/cm² have been measured using Faraday rotation with picosecond resolution. A high density plasma jet has been observed simultaneously with the magnetic fields by interferometry and optical emission. Two-dimensional magnetohydrodynamic simulations reproduced the main features of the experiment and showed that the jet formation is due to pinching by the magnetic fields. [S0031-9007(98)06412-6]

PACS numbers: 52.40.Nk, 52.65.Kj, 52.70.Ds, 52.70.Kz

Large spontaneous magnetic fields are generated during the interaction of a powerful laser pulse with a solid target [1,2]. Up to now, experimental measurements of these fields (up to about 1 MG) have been obtained with laser pulses ranging from a few tens of picoseconds [3] to nanoseconds [4], using optical Faraday rotation probing (*polarimetry*). Because of the availability of novel laser systems and their exciting applications [5], the attention of the scientific community has recently focused on the study of the interaction of ultraintense picosecond and subpicosecond pulses with plasmas. In particular, the fast ignitor scheme [6] for inertial confinement fusion has generated great interest in the study of magnetic fields in short-pulse interactions, and of their effects on the pulse propagation [7]. Magnetic field generation in ultraintense interactions have hence been investigated through analytical and computational studies [8–10] that predict very large fields, up to hundreds of MG in the overdense region of an irradiated solid target.

This Letter presents measurements of megagauss magnetic fields resulting from the interaction of a picosecond laser pulse with Al solid targets, at irradiances exceeding 5×10^{18} W/cm². These are the first magnetic field measurements reported in an intensity and pulse duration regime of interest to fast ignitor studies. Optical probing techniques, with a temporal resolution of the order of a picosecond, allowed the temporal and spatial evolution of the fields to be quantitatively determined. Evidence of collimated plasma flow was obtained via interferometric measurements and optical emission. The interaction was modeled with a 2D magnetohydrodynamic (MHD) code using the experimental conditions. The main features of the experiment were only reproduced when Bohm magnetic flux inhibition was invoked in the code. In particular, the computational results showed that the jet formation is due to pinching by the magnetic fields.

The experiment was performed at the Rutherford Appleton Laboratory using the Vulcan Nd:glass laser operating in the chirped pulse amplification (CPA) mode. The targets were Al foils with a thickness of 25 μ m. The

1.054 μ m CPA interaction pulse, 1.5 ps in duration, was focused onto target by an $F/4.5$ off-axis parabola (OAP), in a 12–15 μ m full width at half maximum (FWHM) focal spot. With an average interaction power of 10 TW, an incident irradiance between 5 and 9×10^{18} W/cm² was obtained. The prepulse to main contrast ratio was 10^{-6} . A fraction of the CPA pulse was used as a temporally independent probe to diagnose the plasma. The accuracy in the probe timing was comparable to the pulse duration. For interferometry the probe beam was frequency doubled in a KDP (potassium dihydrogen phosphate) crystal resulting in a wavelength of 0.527 μ m. The magnetic fields were measured using a polarimetric Faraday rotation technique [1,3,4]. For these measurements the probe beam was Raman shifted in ethanol, to a wavelength $\lambda = 0.622$ μ m. This, together with the use of an interference filter, was effective in reducing the plasma emission noise on film. A microscope objective, with an F number of 4, imaged the plasma onto photographic film, with a magnification of 45 and a spatial resolution of a few microns. The density profiles of the plasma were obtained in separate measurements with a Nomarski modified interferometer [11]. Because of refraction of the probe beam off the steep density gradients and absorption close to the critical surface, the probing of the plasma was generally limited to electron densities up to $(1-2) \times 10^{20}$ /cm³. The spatial extent of the preplasma was also checked via optical probing. The region of preplasma with $n_e > n_c/10$ extended for less than 10 μ m from the target surface.

The experiment was simulated using the Eulerian computer code MH2D (described more fully in [12]) that solves the magnetohydrodynamic equations in cylindrical geometry, using the Van Leer method for advection as interpreted by Youngs [13]. The code includes the pressure-driven magnetic source term, resistive diffusion of the magnetic field, and Spitzer thermal conduction with magnetic inhibition. The plasma is treated as a single temperature, fully ionized perfect gas. Laser energy absorption is modeled through inverse bremsstrahlung and resonant absorption (with a 15% energy deposition in the region around the

critical density). Electric currents are limited so that the electron drift velocity $v_D = (\nabla \times B)/\rho$ cannot exceed a given fraction of the thermal velocity v_e . This is done by imposing a correction term to the collision frequency ν_{ei} when $v_D > v_{\text{lim}} = 10c_s \approx (\frac{1}{6}v_e)$, where c_s is the ion sound speed. This correction is due to the onset of ion-acoustic turbulence [14]. Additional transport effects, such as Righi-Leduc and Nernst terms, are ignored, and transport by ions or suprathermal electrons is not included.

Magnetic fields with a maximum amplitude up to a few MG were detected in the experimental measurements. Because of the high temporal resolution of the probe diagnostic, a quantitative measurement of the transient nature of the fields has been obtained for the first time. Interestingly, no Faraday rotation was detected immediately after the interaction, a possible reason being that the fields were still limited to regions not accessible for probing. After 5 ps the typical signatures corresponding to a toroidal field surrounding the laser axis (i.e., a dark and a bright pattern on opposing sides of the axis, in the proximity of the target surface) began to appear. The strongest rotations were detected between 6 and 12 ps after the interaction. Two polarigrams obtained 12 ps after the interaction, with the polarizers set -9° and $+12^\circ$ off normal are shown in Figs. 1(a) and 1(b). As expected, the dark-bright pattern reverses as the angle between the polarizers is changed from a value below 90° to a value above 90° . The sense of rotation is the same as observed in previous measurements in longer pulse regimes [3,4], and is consistent with fields generated by the thermoelectric mechanism [1].

A map of the product $n_e B$ (electron density times magnetic field) in the plasma was obtained by Abel inverting the rotation angle measured off the polarigrams. The B -field amplitude could then be inferred by using an independent measurement of the density. For this purpose, a similar temporal sequence of interferograms, from which the evolution of the plasma density with time could be ob-

tained, was acquired. An interferogram recorded for similar experimental conditions as the Faraday rotation images is shown in Fig. 1(d).

The magnetic field contours obtained from the polarigram of Fig. 1(a) are shown in Fig. 2. The largest fields detected at this time were of the order of 2–3 MG at an electron density of $(3-5) \times 10^{19}/\text{cm}^3$. The maximum field measured at a fixed density ($4 \times 10^{19}/\text{cm}^3$) versus time is shown in Fig. 3. The relatively large errors in the measurements are mainly due to shot-to-shot variations of the laser parameters and, consequently, of the plasma conditions that particularly affect our measurements since the interferograms were taken on separate shots. However, within the error bars of the measurement, the observed field clearly decreases with time. In addition, at 20 ps after the interaction small scale structures begin to appear, breaking up the uniformity of the rotation pattern. Because of this, and also because of the overall decrease of the rotation angle, it becomes difficult to extract a value for the field amplitude from data taken after 20 ps. At 50–60 ps after the interaction, no rotation is detectable above the background noise, meaning that no field larger than 200–300 kG (i.e., the sensitivity of our diagnostic in these experimental conditions) is present in the region of the plasma that could be probed. It should be noted here that, as it can be seen in Fig. 2, the plasma region in which the fields could be measured was limited not only by refraction, but also by self-emission noise in the region close to the laser axis (within 10–20 μm from the laser axis).

To simulate the experiment, the MH2D code was run for an Al foil irradiated with a 1.5 ps pulse at an irradiance of $5 \times 10^{18} \text{ W}/\text{cm}^2$. An exponential density profile with a scale length of 1 μm was used in the initial conditions. The solid density was approximated with a 100 times n_c plasma. The code was sensitive to the setting of various parameters, such as the choice of a $(1 + \omega\tau)^{-1}$ (Bohm) rather than a $(1 + \omega^2\tau^2)^{-1}$ (Braginsky) reduction in heat

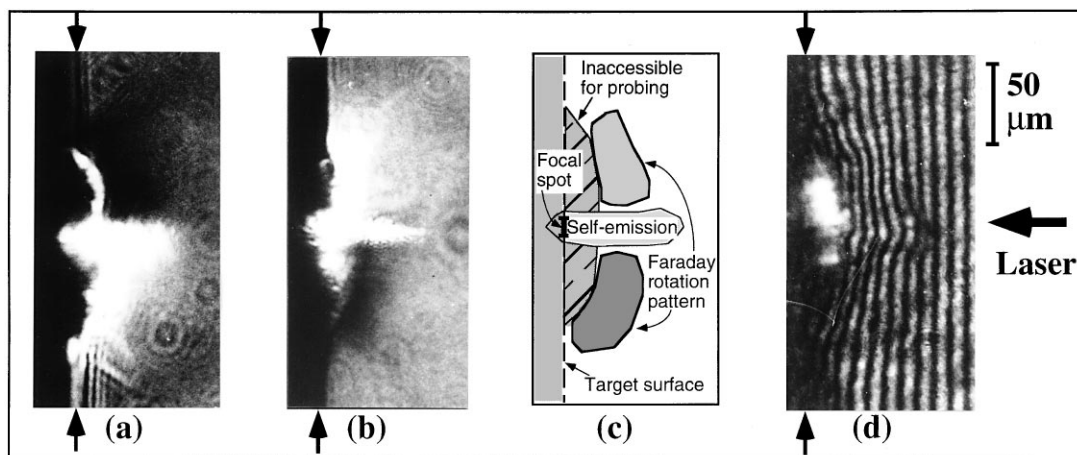


FIG. 1. (a), (b) Polarigrams taken 12 ps after the interaction of a 10 TW, 1.5 ps laser pulse with a solid Al target, with the two polarizers -9° and $+12^\circ$ off crossed. The position of the target surface is indicated by the arrows. (c) Schematic showing the main features of the polarigrams. (d) Interferogram recorded 15 ps after the interaction.

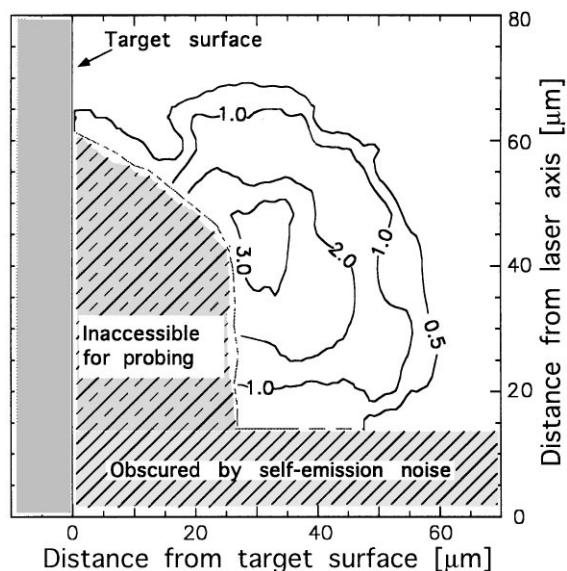


FIG. 2. Magnetic field distribution extracted from the polarigram of Fig. 1(a). The magnitude is in units of megagauss. The plasma region either obscured by self-emission or not accessible for probing is shown.

flow (where ω is the electron gyrofrequency and τ the collision time) [12], or the value of the current limitation velocity v_{lim} . Although the code does not include important processes (such as fast electron and fast ion transport), a purely magnetohydrodynamic treatment of the interaction is, however, sufficient to describe adequately the bulk properties of the plasma expansion. Indeed, the agreement with the experimental observations was remarkable when magnetic inhibition using the Bohm transport reduction term [meaning that the Spitzer conductivity was reduced by a factor proportional to $(1 + \omega\tau)^{-1}$] was imposed. The maximum value of $\omega\tau$ allowable had, however, to be ar-

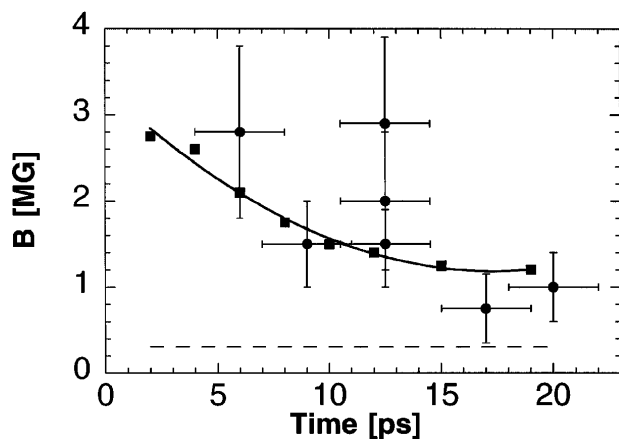


FIG. 3. Temporal evolution of the maximum magnetic field detected at $n_e = 4 \times 10^{19}/\text{cm}^3$ (full circles). The maximum fields predicted at the same density by MHD simulations are also shown (as squares and a solid line). The dashed line corresponds to the sensitivity of the diagnostic.

tificially limited (in this case to 10^4), in order to avoid complete inhibition of the thermal flux from the laser spot region leading to unrealistic temperature values.

The order of magnitude of the fields observed in the simulations, and also their temporal evolution, are in good agreement with the experimental observations. The maximum predicted values at the fixed density of $4 \times 10^{19}/\text{cm}^3$ are plotted for different times in Fig. 3 together with the experimental data. In the simulation the overall peak field (6 MG) is observed at the end of the laser pulse, at densities between $1n_c$ and $5n_c$. The several convective and diffusive processes that can in principle be responsible for the field dissipation are discussed in Ref. [2]. According to the computational results, the magnetic fields observed are consistent with the conventional thermoelectric source. Other generation mechanisms, however, are expected to be responsible for the generation of magnetic fields up to hundreds of MG in the conditions of the reported experiment. For example, particle-in-cell simulations by Wilks *et al.* [8] predict, for a laser pulse interacting with an overdense plasma at an incident irradiance of $5 \times 10^{18} \text{ W}/\text{cm}^2$, the generation of magnetic fields up to 250 MG (a theoretical model for the generation of such fields is given by Sudan [9]). It is interesting to note that the fields here reported are 2 orders of magnitude smaller and appear to be consistent with conventional $\nabla n \times \nabla T$ mechanisms. Even though these observations were limited to the underdense region of the plasma, in principle one would expect large fields generated in the overdense plasma to convect out as the plasma expands and to be observable (though with reduced amplitude) in the coronal plasma after some time. Therefore, it seems that “non-conventional” mechanisms do not contribute significantly to the generation of the fields detected in these experimental conditions.

An important feature immediately evident from the polarigrams [particularly in Fig. 1(b)] is a characteristically elongated self-emission plume, extending up to $100 \mu\text{m}$ from the target surface, with a transverse dimension of $10\text{--}20 \mu\text{m}$. This time-integrated emission at $\lambda = 0.622 \mu\text{m}$ can be interpreted as bremsstrahlung radiation from a dense, collimated plasma plume. Similar structures have previously been reported in different interaction regimes, in x-ray images [12], and in interferograms [3]. The formation of a plume structure in the plasma has also been observed interferometrically. A localized fringe shift, corresponding to a high density jet, is clearly visible in the interferogram of Fig. 1(d), obtained 15 ps after the interaction. The corresponding density distribution [Fig. 4(a)] shows that the density inside the plume is as high as $10^{20}/\text{cm}^3$ out to $80 \mu\text{m}$ from the target surface.

The formation of a jetlike structure in the simulations is characteristic of the interaction in the intensity regime investigated, and the features of the experimental data are overall well reproduced in the computational results. In Fig. 4(b), a contour plot of the density distribution of the

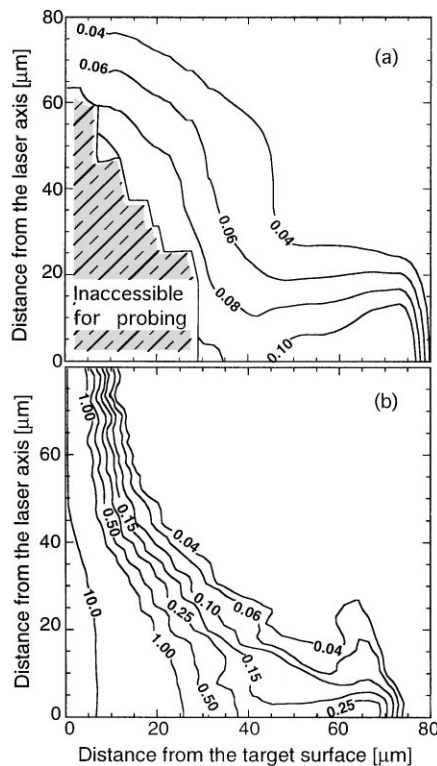


FIG. 4. (a) Electron density distribution extracted from the interferogram of Fig. 1(d). (b) MHD code prediction for the density distribution. The densities given are in units of the critical density ($10^{21}/\text{cm}^3$).

plasma predicted by the code 15 ps after the interaction is shown. A jetlike structure, similar to the one observed experimentally (though with some differences in the density levels and in the transverse size), is clearly visible. Magnetic fields in the range 1–2 MG are predicted to surround the region where the jet is present. The simulations confirm that the jet is formed due to pinching of the plasma by these fields. In fact, if in the code the baroclinic source term for the magnetic field is turned off, no jet formation is observed. A measure of the effectiveness of magnetic confinement can be obtained by the parameter $\beta = 8\pi k_B n_e T_e / B^2$, i.e., the ratio between magnetic and thermal pressure, where k_B is the Boltzmann constant and T_e is the electron temperature. Using values of the order of the experimental and computational results, such as, for example, $n_e = 10^{20}/\text{cm}^3$, $T_e = 3 \text{ keV}$, $B = 3 \text{ MG}$, one obtains $\beta \approx 1$. In other words, magnetic and thermal pressure are of the same order of magnitude, and small variations of the plasma parameters may cause the magnetic pressure to dominate.

In conclusion, MG magnetic fields generated during the interaction of a 10 TW, ps pulse with Al solid targets have been measured, using a polarimetric technique with picosecond temporal resolution. These are the first magnetic field measurements reported in the high intensity regime of interest for fast ignitor applications. The high resolution of the diagnostic allowed the temporal evolution of the fields to be quantitatively studied for the first time. The fields, consistent with the thermoelectric generation mechanism, are transient, with a lifetime of a few tens of picoseconds and affect the plasma expansion, confining it to a collimated plume. A 2D MHD code was run for the conditions of the experiment, resulting in the first direct comparison between experimental data and magnetohydrodynamic simulations in laser produced plasmas. The main features of the experimental observations were reproduced by the code, demonstrating that the jet is formed due to pinching by the magnetic fields.

The authors acknowledge the support received by the staff of the Central Laser Facility (Rutherford Appleton Laboratory). This work was funded by an EPSRC/MoD grant. One of the authors (A. J. MacK.) was supported by a Lawrence Livermore National Laboratory contract.

-
- [1] J. A. Stamper, *Laser Part. Beams* **9**, 841 (1991).
 - [2] M. G. Haines, *Phys. Rev. Lett.* **78**, 254 (1997).
 - [3] M. D. J. Burgess *et al.*, *Phys. Fluids* **28**, 2286 (1985).
 - [4] J. A. Stamper and B. H. Ripin, *Phys. Rev. Lett.* **34**, 138 (1975); A. Raven, O. Willi, and P. T. Rumsby, *Phys. Rev. Lett.* **41**, 554 (1978); O. Willi, P. T. Rumsby, and C. Duncan, *Opt. Commun.* **37**, 45 (1981).
 - [5] P. Gibbon and E. Forster, *Plasma Phys. Controlled Fusion* **38**, 769 (1996).
 - [6] M. Tabak *et al.*, *Phys. Plasmas* **1**, 1626 (1994).
 - [7] A. Pukhov and J. Meyer-ter Vehn, *Phys. Rev. Lett.* **76**, 3975 (1996).
 - [8] S. C. Wilks *et al.*, *Phys. Rev. Lett.* **69**, 1383 (1992).
 - [9] R. N. Sudan, *Phys. Rev. Lett.* **70**, 3075 (1993).
 - [10] F. Brunel, *Phys. Fluids* **31**, 2714 (1988); H. Ruhl and P. Mulser, *Phys. Lett. A* **205**, 388 (1995).
 - [11] R. Benattar, C. Popovics, and R. Sigel, *Rev. Sci. Instrum.* **50**, 1583 (1979).
 - [12] A. R. Bell *et al.*, *Phys. Rev. E* **48**, 2087 (1993); A. R. Bell, *Phys. Plasmas* **1**, 1643 (1995).
 - [13] D. L. Youngs, *Numerical Methods in Fluid Dynamics*, edited by K. W. Morton and M. J. Baines (Academic, New York, 1982).
 - [14] W. M. Manheimer, *Phys. Fluids* **20**, 265 (1977).